

## ***Supporting Information***

# **Positive Effect of the Residual Templates within the MCM-41 Mesoporous Silica Channels in the Metal-Catalyzed Catalytic Reactions**

**Kohsuke Mori<sup>a,b\*</sup>, Takuya Yamaguchi<sup>a</sup>, Shohei Ikurumi<sup>a</sup> and Hiromi Yamashita<sup>a,b\*</sup>**

<sup>a</sup> Division of Materials and Manufacturing Science, Graduate School of Engineering, Osaka University, 2-1 Yamada-oka, Suita, Osaka 565-0871, Japan. Fax & Tel: +81-6-6879-7457, E-mail: mori@mat.eng.osaka-u.ac.jp, yamashita@mat.eng.osaka-u.ac.jp

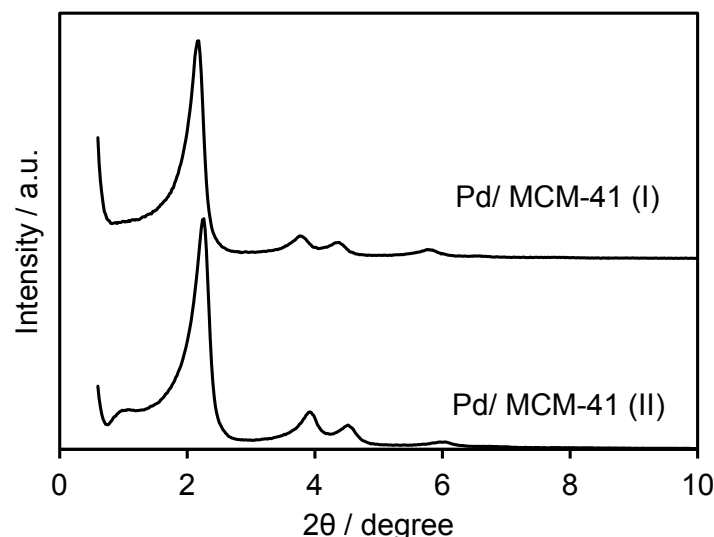
<sup>b</sup> Unit of Elements Strategy Initiative for Catalysts & Batteries, Kyoto University, Katsura, Kyoto 615-8520, Japan

## **1. Experimental**

**1.1. Characterization:** Powder X-ray diffraction patterns were recorded using a Rigaku Ultima IV diffractometer with Cu K $\alpha$  radiation ( $\lambda = 1.5406 \text{ \AA}$ ). Reflectance spectra were collected using a Shimadzu UV-2450 spectrophotometer. The elemental composition was determined by inductively coupled plasma (ICP) analysis using a Nippon Jarrell-Ash ICAP-575 Mark II. BET surface area measurements were performed using a BEL-SORP max (Bel Japan, Inc.) at 77 K. The sample was degassed in vacuum at 343 K for 24 h prior to data collection. TG analysis was carried out by a Rigaku Thermo Plus EVO II. Infrared spectra were obtained with a JASCO FTIR-6100. Samples were diluted with KBr and compressed into thin disk-shaped pellets. TEM micrographs were obtained with a Hitachi Hf-2000 FE-TEM equipped with a Kevex energy-dispersive X-ray detector operated at 200 kV. Pd K-edge XAFS spectra were recorded using a fluorescence-yield collection technique at the beam line 01B1 station with an attached Si (311) monochromator at SPring-8, JASRI, Harima, Japan (prop. No. 2012A1061 and 2012B1058). The EXAFS data were normalized by fitting the background absorption coefficient, around the energy region higher than the edge of about 35–50 eV, with the smoothed absorption of an isolated atom. The EXAFS data were examined using the Rigaku EXAFS analysis program. Fourier transformation (FT) of  $k^3$ -weighted normalized EXAFS data was performed over the  $3.5 \text{ \AA} < k/\text{\AA}^{-1} < 11 \text{ \AA}$  range to obtain the radial structure function.

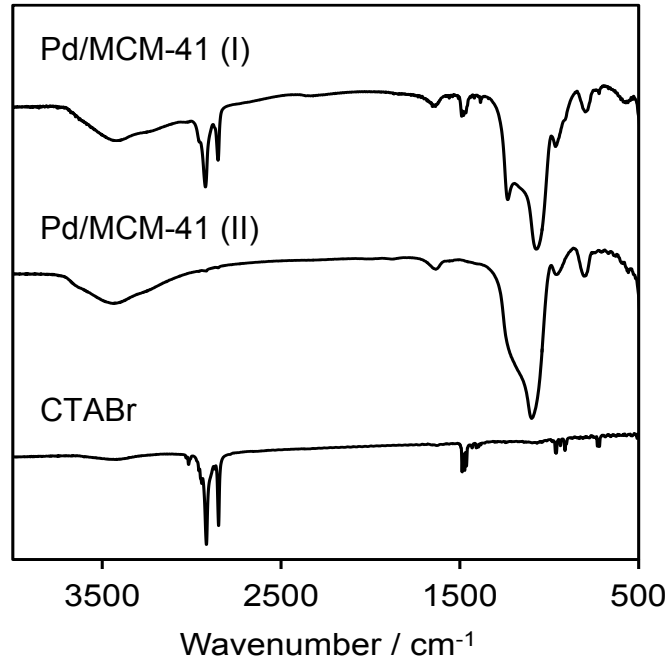
**1.2. Synthesis of Pd/MCM-41(I):** Mesoporous silica (MCM-41) was prepared by a previously reported method. The MCM-41 obtained was washed with deionized water (2 L) and dried under vacuum before further treatment. The as-synthesized MCM-41 (0.5 g) without calcination underwent template-ion exchange (TIE) treatment with an aqueous  $(\text{NH}_4)_2\text{PdCl}_4$  solution (0.4 mM, 50 mL) for 1 h with stirring and kept at 353 K for *ca.* 20 h. The resultant solid was recovered by filtration, washed with deionized water (1 L), and dried under vacuum. Finally, reduction with an aqueous  $\text{NaBH}_4$  solution (2.8 mM, 25 mL) in an Ar atmosphere followed by filtration, washing with water (1 L), and drying under vacuum, afforded Pd/MCM-41 (Pd 0.5 wt%). In order to reproduce the sample, special attention should be paid in the washing process.

## 2. XRD



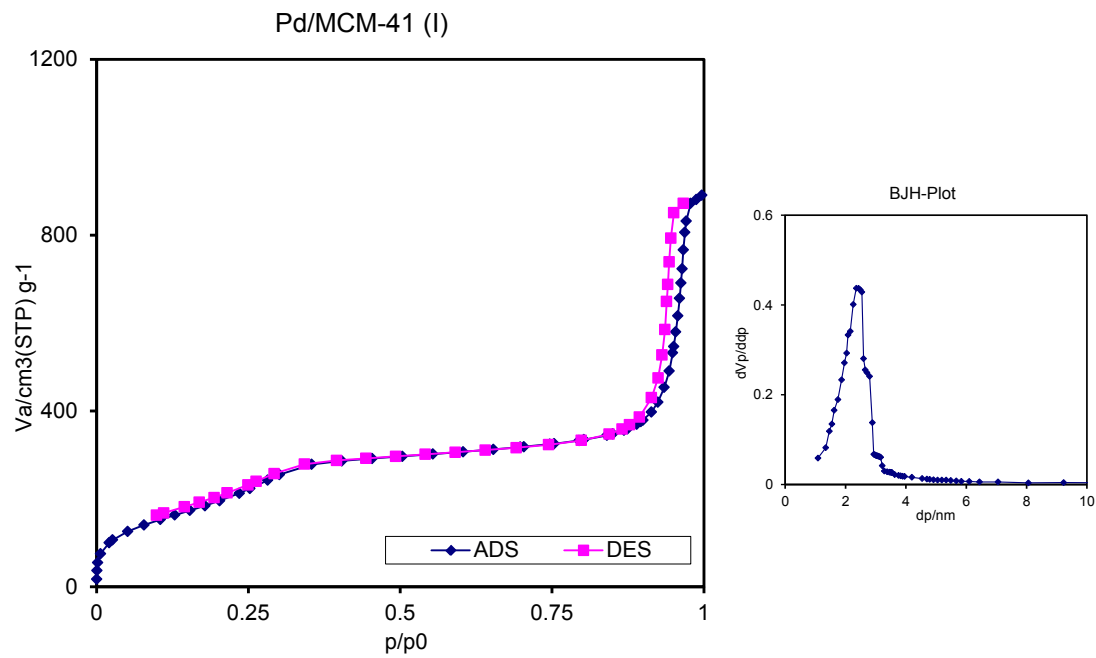
**Figure S1** XRD Pattern of as-synthesized Pd/MCM-41 (I) and calcined Pd/MCM-41(II).

### 3. FT-IR



**Figure S2** FT-IR spectra of as-synthesized Pd/MCM-41 (I), calcined Pd/MCM-41(II) and cetyltrimethylammonium bromide (CTABr).

### 4. N<sub>2</sub> adsorption-desorption isotherms



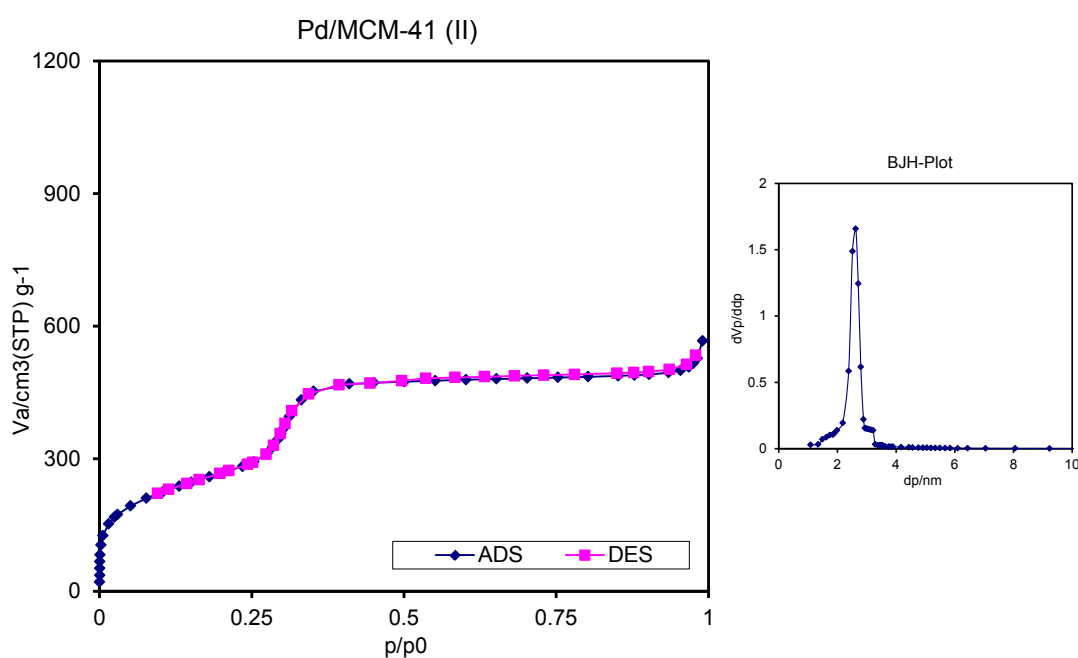


**Figure S3** N<sub>2</sub> adsorption-desorption isotherms and pore diameter of Pd/MCM-41 (I) and Pd/MCM-41 (II).

## 5. TG analysis

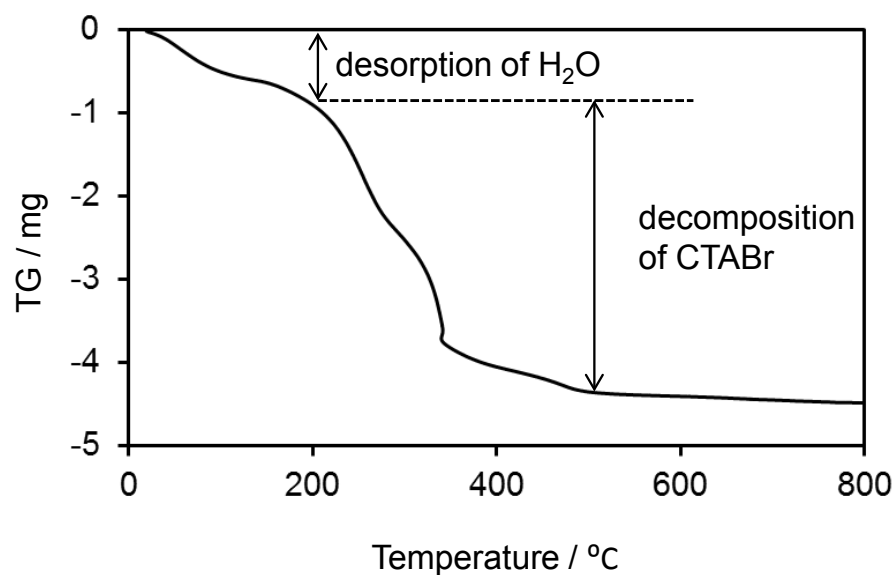


**Figure S4** TG analysis of as-synthesized Pd/MCM-41 (I).

## 6. TEM

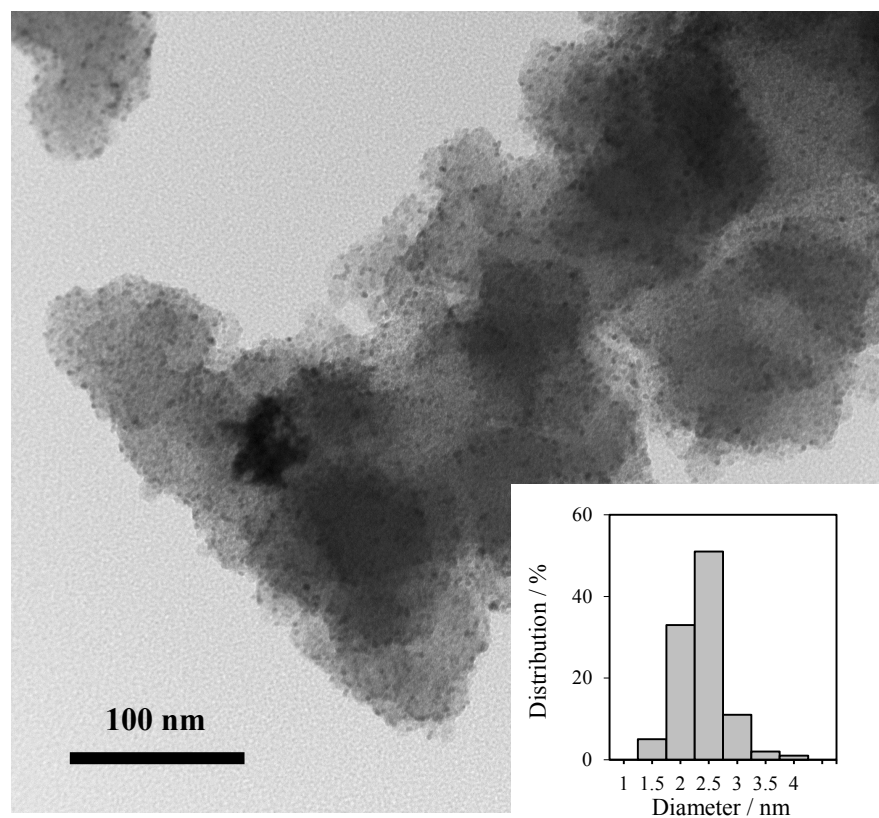


**Figure S5** TEM image and size distribution diagrams of as-synthesized Pd/MCM-41(i)<sup>c</sup>.